Acta Biochim Biophys Sin 2013, 45: 408–415 | © The Author 2013. Published by ABBS Editorial Office in association with Oxford University Press on behalf of the Institute of Biochemistry and Cell Biology, Shanghai Institutes for Biological Sciences, Chinese Academy of Sciences. DOI: 10.1093/abbs/gmt024.
Advance Access Publication 26 March 2013

Original Article

Blocking the butyrate-formation pathway impairs hydrogen production in *Clostridium perfringens*

Ruisong Yu[1,3], Ruofan Wang[1], Ting Bi[2], Weining Sun[2], and Zhihua Zhou[1*]

[1]Key Laboratory of Synthetic Biology, Institute of Plant Physiology and Ecology, Shanghai Institutes for Biological Sciences, Chinese Academy of Sciences, Shanghai 200032, China
[2]National Key Laboratory of Plant Molecular Genetics, Institute of Plant Physiology and Ecology, Shanghai Institutes for Biological Sciences, Chinese Academy of Sciences, Shanghai 200032, China
[3]Shanghai Key Laboratory of Agricultural Genetics and Breeding, Institute of Animal Husbandry and Veterinary Science, Shanghai Academy of Agricultural Sciences, Shanghai 201106, China
*Correspondence address. Tel: +86-21-54924050; Fax: +86-21-54924049; E-mail: zhouzhihua@sippe.ac.cn

Inactivating competitive pathways will improve fermentative hydrogen production by obligate anaerobes, such as those of genus *Clostridium*. In our previous study, the hydrogen yield of *Clostridium perfringens* W13 in which L-lactate dehydrogenase was inactivated increased by 44% when compared with its original strain W12. In this study, we explored whether blocking butyrate formation pathway would increase hydrogen yield. The acetyl-CoA acetyltransferase gene (*atoB*) encodes the first enzyme in this pathway, which ultimately forms butyrate. *Clostridium perfringens* W14 and W15 were constructed by inactivating *atoB* in W13 and W12, respectively. The hydrogen yield of W14 and W15 was 44% and 33% of those of W13 and W12, respectively. Inactivation of *atoB* decreased the pyruvate synthesis and its conversion to acetyl-CoA in both mutants, and increased ethanol formation in W14 and W15. Proteomic analysis revealed that the expressions of five proteins involved in butyrate formation pathway were up-regulated in W14. Our results suggest that butyrate formation deficiency improved ethanol production but not hydrogen production, indicating the importance of butyrate formation pathway for hydrogen production in *C. perfringens*.

Keywords *Clostridium perfringens*; two-dimensional gel electrophoresis; biohydrogen; butyrate; ethanol

Received: November 6, 2012 Accepted: December 25, 2012

Introduction

Biological production of hydrogen by different microorganisms has been attracting interest due to concerns regarding the environmentally benign alternatives to current fossil energy sources [1,2]. Since other reducing metabolites, such as propionate, butyrate, and sometimes lactate and ethanol, are produced during anaerobic fermentation, the hydrogen yields of dark fermentation have been reported to range from 0.6 to 1.9 mol/mol glucose [3–6], which are substantially less than the theoretical yield (4 mol/mol glucose). Previous studies have attempted to improve hydrogen yield by engineering related metabolic pathways, particularly those related to the composition of liquid metabolites [7–13].

The hydrogen yield was enhanced from 1.08 to 1.82 mol/mol glucose by eliminating lactate and succinate formation in an *ldhA* (lactate dehydrogenase gene) and *frdBC* (fumarate reductase gene) double-mutant *Escherichia coli* SR15 stain. In this strain, the yield of acetate was also enhanced by 34% [7]. The hydrogen yield in a *Klebsiella oxytoca* mutant in which bifunctional acetaldehyde-CoA/alcohol dehydrogenase gene (*adhE*) was inactivated increased by 16% and its ethanol concentration decreased by 77% [8]. Similar metabolic engineering studies have been performed in *Enterobacter* species. A *hycA* and *hybO* (encoding formate hydrogen lyase repressor protein and uptake hydrogenase small subunit, respectively) double-mutant, *Enterobacter aerogenes* IAM1183-AO, yielded 1.36 mol hydrogen/mol glucose (1.17 times greater than the wild type), and the yields of lactate, acetate, and ethanol were also increased [4]. The hydrogen yield in an *Enterobacter cloacae* strain increased by 1.5 times (to 3.4 mol/mol glucose) when its alcohol and organic acid formation pathways were blocked; however, no significant effects on acetate yield were observed [9].

Some *Clostridium* strains have been genetically engineered to improve hydrogen production. Overexpression of [FeFe]-hydrogenase in *Clostridium paraputrificum* M-21 resulted in a 1.7-fold hydrogen yield increase from 1.4 to 2.4 mol/mol GlcNAc. Meanwhile, acetate yield

increased and lactate production reduced significantly [10]. Inactivation of *ack* (encoding acetate kinase), thus inactivating the acetate formation pathway in *Clostridium tyrobutyricium*, enhanced hydrogen and butyrate production from glucose. However, no significant effect on acetate formation was identified [11]. In a previous study with the same strain, inactivation of *pta*, encoding phosphotransacetylase which is another key enzyme in the acetate formation pathway, had little effect on hydrogen production. However, this inactivation had the same effects on butyrate and acetate production as *ack* inactivation [12]. In our previous study, the hydrogen yield in a *C. perfringens* mutant (W13) with an inactivation of *ldh* gene (encoding L-lactate dehydrogenase, **Fig. 1**) increased 44% since the lactate formation pathway was completely blocked. Concentrations of acetate and butyrate in its fermentation effluent increased 26% and 57%, respectively [13].

In this study, we inactivated the butyrate formation pathway and monitored the effects on hydrogen production in *C. perfringens*. Proteomic analysis of *C. perfringens* mutants was performed to determine the biological mechanisms of changes in hydrogen production.

Materials and Methods

Bacterial strains, plasmids, and growth conditions

Clostridium perfringens W12 and its mutants were precultured in modified liquid growth medium for the genus *Clostridium* (CGM). For hydrogen production, 0.5 ml of *C. perfringens* preculture was inoculated into 28 ml of hydrogen-producing medium in 38 ml anaerobic tubes as described previously [13]. The hydrogen-producing medium contained 1.5 g/l KH_2PO_4, 4.2 g/l $Na_2HPO_4{\cdot}12H_2O$, 0.18 g/l $MgCl_2{\cdot}6H_2O$, 0.1 g/l $FeSO_4{\cdot}7H_2O$, 2 g/l yeast extract, 1 g/l glutamic acid, and 10 g/l sucrose. Tubes sealed with rubber stoppers were kept at 37°C for 48 h and 60 ml of syringes were used to collect and measure biogas production.

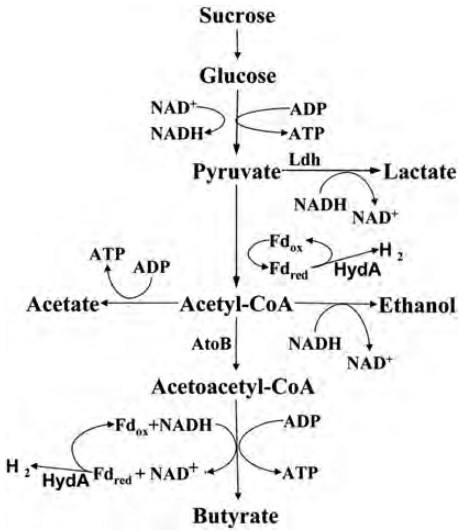

Figure 1 Schematic diagram of the central metabolic pathway in *C. perfringens* Ldh, lactate dehydrogenase; HydA, hydrogenase; AtoB, acetyl-CoA acetyltransferase; Fd_{ox}, oxidized ferredoxin; Fd_{red}, reduced ferredoxin.

PMD18-T (TaKaRa, Tokyo, Japan) was used as a cloning and sequencing vector for *E. coli.* The *E. coli*–*C. perfringens* shutter vector pJIR750ai (Sigma-Aldrich, St Louis, USA) was chosen as the TargeTron gene knock out plasmid. *Escherichia coli* TOP 10 was used as clone host and grown at 37°C in Luria–Bertani (LB) medium supplemented with ampicillin (100 μg/ml) or chloramphenicol (25 μg/ml).

The cell density was determined by measuring absorbance at 600 nm. For biomass measurements, 20 ml of fermentation broth samples were centrifuged at 12,000 × *g* for 10 min, and pellets were washed three times with physiological saline and weighed after drying at 60°C for more than 48 h.

DNA extraction

Plasmid DNA from *E. coli* was isolated using Axygen plasmid Miniprep kit (Axygen, Union, USA) and genome DNA of *C. perfringens* strains were prepared using Wizard Genomic DNA purification kit (Promega, Madison, USA) as described previously [13]. DNA fragments were purified from gel using gel extraction kit (Axygen).

Construction of *C. perfringens* W14 and W15

Full-length *atoB* from *C. perfringens* was amplified using polymerase chain reaction (PCR) primers aotB-F and atoB-R (**Table 1**) and was confirmed by sequencing. The sequence was then submitted to the TargeTron design site (http://www.sigma-aldrich.com/targetronaccess) to predict intron insertion sites. The insertion site at position 411/412 from initial ATG in anti-sense strand was chosen for intron modification. Modifications of intron RNA sequences with *atoB* target site sequences were performed by PCR using three *atoB* gene-specific primers atoB411|412a-IBS, atoB411|412a-EBS1d and atoB411|412a-EBS2 (**Table 1**). The amplified 350 bp fragment digested with *Hin*dIII and *Bsr*GI was ligated into pJIR750ai (digested with same two restriction enzymes) to construct recombinant plasmid pJIR750-atoB.

The vector pJIR750-atoB was then electroporated into *C. perfringens* W13 and W12 to obtain W14 and W15, respectively. Chloramphenicol-resistant colonies were screened for TargeTron insertion by PCR using primers atoB-41F and atoB-451R (**Table 1**), and for further confirmation, amplified fragments were cloned into pMD19-T (TaKaRa) for sequencing just as in other studies [14,15].

Table 1 Primers used in this study

Primer	Sequence (5′→3′)
AtoB-F/AtoB-R	ATGAGAGAGGTAGTTATT/TTATCTTTCTACTATTAAA
AtoB-41F/AtoB-451R	TAGGTTCATTTGGTGGTT/CATCTGTTAAAGCGTCAT
411|412a-IBS	AAAAAAGCTTATAATTATCCTTAATCAACCATTTTGTGCGCCCAGATAGGGTG
411|412a-EBS1d	CAGATTGTACAAATGTGGTGATAACAGATAAGTCCATTTTTCTAACTTACCTTTCTTTGT
411|412a-EBS2	TGAACGCAAGTTTCTAATTTCGGTTTTGATCCGATAGAGGAAAGTGTCT
EtfA-F/EtfA-R	GGTGGTAGAGGTATTGGT/TGTTGAATAGCTCCTGAT
EtfB-F/EtfB-R	AAGTATGGGACCACCTCA/TTCTGGACCAACCTGTGC
Crt-F/Crt-R	TAGACAAGCCTGTAATCG/GAGTTCCACCAAATCCTG
Buk-F/Buk-R	GATCAATGGCTGTAGTTT/TCATCTTCTCCACCGTAT
Ptb-F/Ptb-R	ATCCTAATATGCCAGCAA/CCAACTAATAACCCACCA
16S-F/16S-R	ACAAGGTGACAGGTGGTG/TCAGCCTACAATCCGAAC
Adh-F/Adh-R	TAAACCAAACCCAACAGT/TAGCGAATAAAGTCATCTCA
AdhE-F/AdhE-R	AAGTTACTCCAGACCCAA/TGCTCATACATTACCCAC

AtoB, acetyl-CoA acetyltransferase; EtfA and EtfB, electron transfer flavoprotein alpha and beta subunit, respectively; Crt, 3-hydroxybutyryl-CoA dehydratase; Ptb, phosphate butyryltransferase; Buk, butyrate kinase; Adh, alcohol dehydrogenase; AdhE, bifunctional acetaldehyde-CoA/alcohol dehydrogenase; 16S, 16S rRNA.

Metabolite analysis

The composition of the evolved biogas (mainly H_2 and CO_2), alcohols, and organic acids were determined as described previously [13]. Briefly, the composition of evolved biogas was determined in a gas chromatograph (GC) (GC7900; Techcomp, Shanghai, China) equipped with a thermal conductivity detector. Alcohols in fermentation effluents were quantified by GC (17A; Shimadzu, Kyoto, Japan) with a flame ionization detector and a 30-m FFAP capillary column. Organic acids in fermentation effluents were quantified by high-performance liquid chromatography (Shimadzu) with two Shodex RSpak KC-811 ion exchange columns (8 by 300 mm).The volume of hydrogen gas produced was converted to normal conditions. Hydrogen yield was calculated as the ratio of the moles of H_2 produced to the moles of equivalent hexose to sucrose added. All data, including hydrogen yield, concentration of fatty acids were mean values of at least three replication.

Proteomic analysis

For proteomic analysis, *C. perfringens* W12, W13, and W14 stains were harvested for ~12 h after inoculation to hydrogen-producing medium. Two-dimensional polyacrylamide gel electrophoresis (2-DE) followed by mass spectrometric analysis was employed as described previously [16]. Briefly, pelleted cells were washed in TE buffer, resuspended in lysis buffer, and lysed by sonication. A protein aliquot (120 μg) from each sample was subjected to 2-DE. The silver-stained gels were scanned and analyzed using Progenesis SameSpots software (Nonlinear, Newcastle, UK). Protein spots were excised and submitted to in-gel-digestion prior mass spectrometric (MS) analysis. MS and tandem mass spectrometric (MS/MS) analysis were performed using a 4700 proteomics analyzer (Applied Biosystems, Framingham, USA). MS and MS/MS data were analyzed using MASCOT 2.1 software (Matrix Science, London, UK) to search against NCBInr database.

Gene expression analysis by quantitative real-time reverse transcriptase (RT)-PCR

To validate gene expression variations related to butyrate metabolism at transcriptional level, real-time reverse transcriptase (RT)-PCR was performed. Primers used for real-time RT-PCR assay are listed in **Table 1**. During late exponential growth phase (12 h after inoculation), 1 ml of W12, W13, or W14 culture was collected for total RNA extraction, and then real-time RT-PCR was performed as described previously [17]. Gene expression level was normalized to that of corresponding 16S rRNA.

Statistical analysis

Data were analyzed using Students *t*-test. $P < 0.05$ was considered as statistically significant.

Results

Growth of *C. perfringens* W14 and W15

The TargeTron vector pJIR750-atoB was electroporated into *C. perfringens* strains W13 and W12 to produce W14 and W15, respectively. Positive colonies were identified based on the presence of a 1300-bp fragment band, while the length of corresponding fragment in parent strain was 410 bp (data not shown). The *atoB*-intron was detected in sequenced PCR fragments from W14 and W15, indicating

that intron was integrated into the site between nt 411and 412 of *atoB*, and thus inactivated AtoB in W14 and W15 (data not shown).

The growth curves of *C. perfringens* W14 and W15 were similar to those of W12 and W13 [**Fig. 2(A)**]. The specific growth rate in *C. perfringens* W12, W13, W14, and W15 was 1.62 ± 0.35/h, 1.43 ± 0.37/h, 1.56 ± 0.43/h, and 1.41 ± 0.53/h, respectively. The cell biomass of these four strains was also similar and reached ~0.5 g/l (dry weight).

Production of hydrogen and other metabolites

As described in our previous study [13], the inactivation of *ldh* increased hydrogen yield by 42% and decreased lactate yield to nearly zero in W13 [**Table 2**, **Fig. 2(D,H)**]. Although the inactivation of *atoB* in W14 and W15 decreased butyrate yield to zero as expected [**Fig. 2(G)**], hydrogen production decreased in both W14 and W15 [**Table 2**, **Fig. 2(D)**]. The hydrogen yield in W15 was 0.56 mol/mol hexose, only 33% of that in W12. The hydrogen yield in W14 was 1.07 mol/mol hexose, which was ~44% of that in W13. Similarly, the hydrogen production rates of W14 and W15 decreased significantly (data not shown). After hydrogen production stopped, W12 and W13 consumed added sucrose, while W14 and W15 consumed only 56% and 63% of added sucrose, respectively [**Fig. 2(B)**].

In W12 and W13, pyruvate accumulated, peaked at 16 h, and decreased nearly to zero when hydrogen production stopped at 44 h [**Fig. 2(E)**]. In W14, pyruvate accumulated during entire fermentation period. The acetate yield in W14 was only 80% of that in W12 [**Fig. 2(F)**]. In contrast, its ethanol yield increased ~10-fold when compared with W12 and W13, which was the highest in all strains examined [**Fig. 2(I)**]. The metabolic flux, including reductive ability stored from butyrate and lactate formation, shifted the pathway to ethanol formation and blocked pyruvate consumption.

When only butyrate formation pathway was blocked (as in W15), less pyruvate accumulated and its initial consumption time started after 4 h [**Fig. 2(E)**]. Acetate accumulation

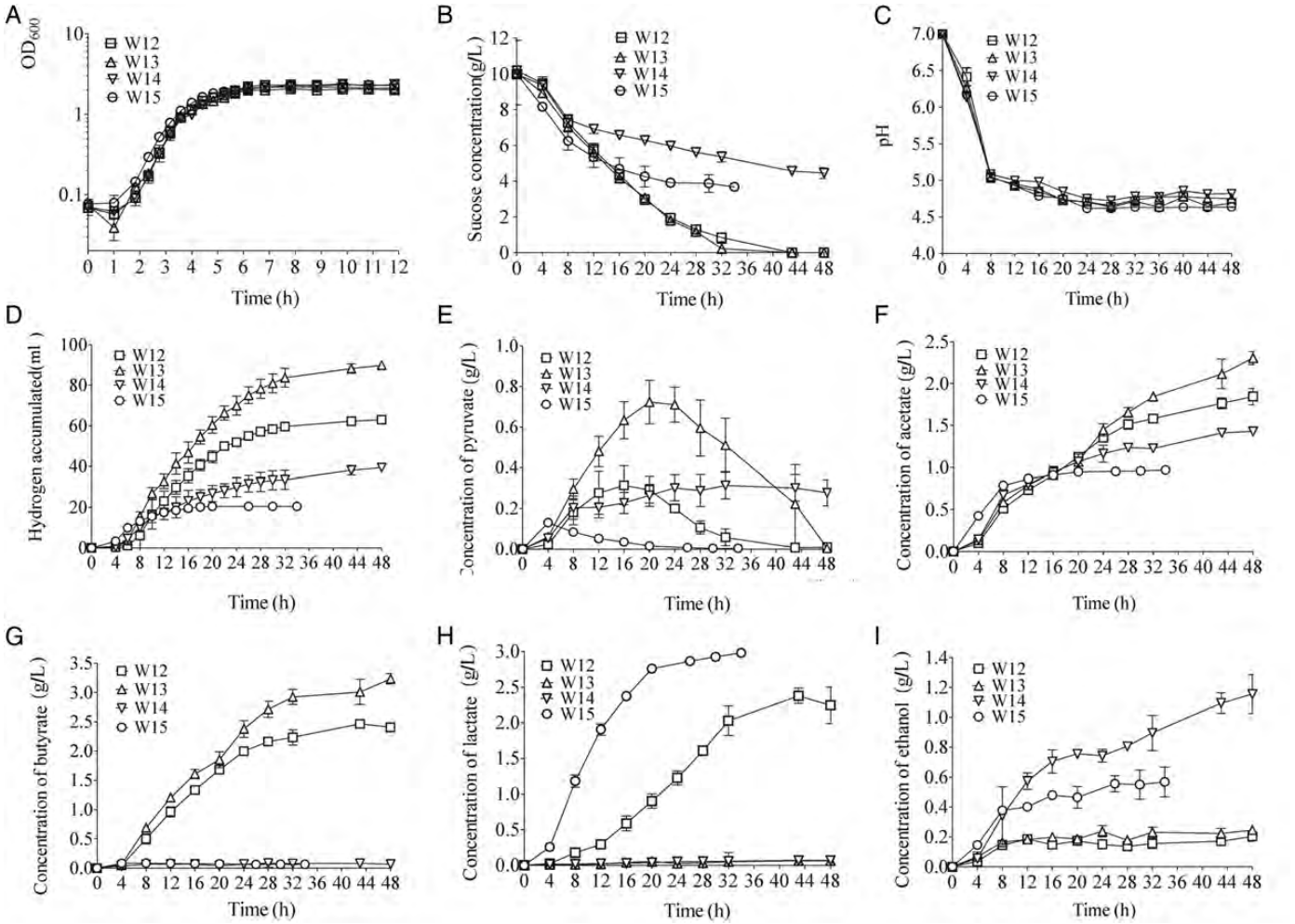

Figure 2 Growth curves and fermentation profiles of *C. perfringens* W12 and its mutants using 10 g/l sucrose as carbon source Growth curve (A), sucrose consumption (B), pH variation (C), and profiles of cumulated hydrogen (D), pyruvate (E), acetate (F), butyrate (G), lactate (H), and ethanol (I) of *C. perfringens* W12 and its mutants. W12, Δ*plc* (encoding alpha toxin); W13, Δ*plc*/Δ*ldh* (encoding lactate dehydrogenase); W14, Δ*plc*/Δ*ldh*/Δ*atoB* (encoding acetyl-CoA acetyltransferase); W15, Δ*plc*/Δ*atoB*.

Table 2 Comparison of the fermentation results in hydrogen production process by *C. perfringens* mutants

Fermentation result	Strain			
	W12	W13	W14	W15
H_2 (ml)	63.0 ± 1.7	89.8 ± 0.3	39.4 ± 0.9	20.5 ± 1.5
Acetate (g/l)	1.85 ± 0.10	2.31 ± 0.08	1.43 ± 0.09	0.97 ± 0.03
Butyrate (g/l)	2.41 ± 0.08	3.23 ± 0.09	0	0
Ethanol (g/l)	0.20 ± 0.03	0.25 ± 0.02	1.16 ± 0.13	0.57 ± 0.10
Lacatate (g/l)	2.25 ± 0.25	0	0	2.98 ± 0.03
Final pH	4.69 ± 0.01	4.75 ± 0.01	4.82 ± 0.02	4.64 ± 0.01
Residue sucrose (g/l)	0	0	4.45	3.68
Calculated carbon balances[a]	1.02	1.04	0.94	0.94
Calculated redox balances[b]	0.86	0.93	0.99	0.84

W12, Δ*plc* (encoding alpha toxin); W13, Δ*plc*/Δ*ldh* (encoding lactate dehydrogenase); W14, Δ*plc*/Δ*ldh*/Δ*atoB* (encoding acetyl-CoA acetyltransferase); W15, Δ*plc*/Δ*atoB*.

[a]Carbon balance = $(\text{sucrose}_{\text{butyrate}} + \text{sucrose}_{\text{acetate}} + \text{sucrose}_{\text{lactate}} + \text{sucrose}_{\text{ethanol}} + \text{sucrose}_{\text{residue}})/\text{sucrose}_{\text{added}}$.

[b]Redox balances = $(\text{NADH}_{\text{butyrate}} + \text{NADH}_{\text{lactate}} + \text{NADH}_{\text{ethanol}} + \text{NADH}_{\text{H2}})/\text{NADH}_{\text{sucrose (produced from sucrose to pyruvate)}}$.

decreased 48% while the accumulation of lactate and ethanol increased 32% and 185%, respectively, when compared with W12. The concentration of lactate increased faster than that of ethanol [**Fig. 2(H,I)**]. The metabolic flux stored from butyrate formation shifted to lactate formation followed by ethanol formation.

Proteomic analysis of *C. perfringens* W12 and its mutants W13 and W14

As expected, Ldh and AtoB were absent in proteomes of W13 and W14, respectively. The abundance of all proteins involved in butyrate formation pathway did not differ significantly in W12 and W13. However, the abundance of five proteins, electron transfer flavoprotein alpha (EtfA) and beta (EtfB) subunits, 3-hydroxybutyryl-CoA dehydratase (Crt), phosphate butyryltransferase (Ptb), and butyrate kinase (Buk), which are involved in butyrate formation pathway, increased significantly in W14 proteome (**Fig. 3**, **Table 3**). The abundance ratio of W14 to W12 ranged from 1.9 to 6.3 (**Fig. 3**, **Table 3**). RT-PCR analysis further confirmed that the transcriptional level of these five genes increased more than 1.5 times in W14 when compared with those in W12 and W13 (**Fig. 3**).

Ethanol acts as a substitute for butyrate and is one of the main end products in W14. However, variations of two key enzymes, Adh and AdhE, in ethanol formation pathway were not detected in strains W12–W14. The transcription levels of *adh* and *adhE* were slightly up-regulated in W14 when compared with those in W12 and W13 (**Fig. 3**).

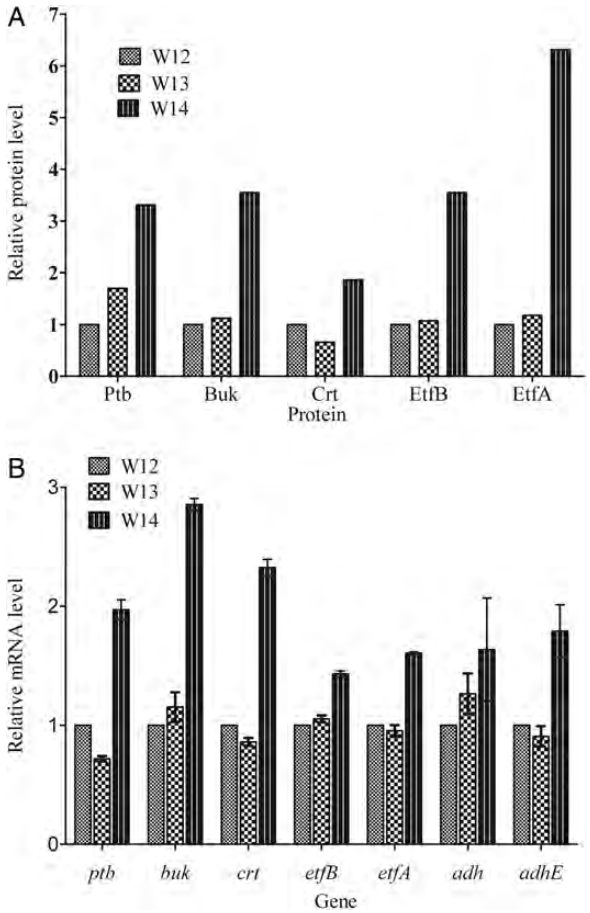

Figure 3 Variations in expression levels of genes involved in butyrate formation pathway as determined by 2-DE (A) and real-time RT-PCR (B) EtfA, electron transfer flavoprotein alpha subunit; etfB, electron transfer flavoprotein beta subunit; crt, enoyl-CoA hydratase; buk, butyrate kinase; ptb, phosphate butyryltransferase; adh, alcohol dehydrogenase; adhE, bifunctional acetaldehyde-CoA/alcohol dehydrogenase. W12, Δ*plc* (encoding alpha toxin); W13, Δ*plc*/Δ*ldh* (encoding lactate dehydrogenase); W14, Δ*plc*/Δ*ldh*/Δ*atoB* (encoding acetyl-CoA acetyltransferase).

Discussion

Blocking lactate and/or butyrate formation pathway had little effect on cell growth in W14 and W15 when compared

Table 3 Classification of differentially expressed proteins in *C. perfringes* W12 and its mutants

Spot ID	Protein description[a]	NCBI accession number	Theor. M_r[b]/pI[c]	Gene locus	Gene	Sequence coverage (%)	Peptides match/ search[d]	Unique peptides detected by MS/MS[e]	Mascot score	Ratio[f]	
										W13/ W12	W14/ W12
1	Electron transfer flavoprotein alpha subunit	gi|18311280	36119/5.04	Cpe2298	*EtfA*	20	9/24	9	178	1.18	6.31
2	Electron transfer flavoprotein beta subunit	gi|18311281	27988/5.30	Cpe2299	*EtfB*	10	6/63	6	100	1.07	3.55
3	Enoyl-CoA hydratase	gi|18311283	28166/4.94	Cpe2301	*Ert*	16	5/36	5	159	0.66	1.86
4	Butyrate kinase	gi|18311329	38621/5.74	Cpe2347	*Buk*	17	8/19	8	110	1.12	3.55
5	Phosphate butyryltransferase	gi|11080939	32240/5.73	Cpe2348	*Ptb*	21	8/24	8	123	1.70	3.31

[a]The protein description was primarily based on the genome annotation of *C. perfringens str.13*.
[b]Theor. M_r is the abbreviation of theoretical molecular mass.
[c]Theor. pI is the abbreviation of theoretical isoelectric point.
[d]Protein identified by peptide mass fingerprint (PMF). The number of peptides that match/searched peptides was provided.
[e]Protein identified by PMF and MS/MS.
[f]Differential protein expression (ratio) of corresponding protein.

with their original strains W13 and W12. In a previous study, the inactivation of butyrate formation pathway had little effect on the growth of *C. butyricum* [18]. However, a study of *C. tyrobutyricium* has revealed that the inactivation of *pta* or *ack* in acetate formation pathway decreases the growth rate of mutants since acetate formation pathway generates more ATP than other pathways during fermentation [12], which suggests that butyrate and lactate formation pathways do not play major roles in energy generation.

Added sucrose was consumed almost completely in W12 and W13. However, a large amount of sucrose remained in the effluent of W14 and W15, in which gene *atoB* had been inactivated [**Table 2, Fig. 2(B)**]. Phosphofructokinase (Pfk) was reported to be the key enzyme regulating the speed of Embden–Meyerhof–Parnas pathway (EMP) [19]. It has been reported that Pfk is sensitive to acidity [20,21] and its activity is completely inhibited at pH $\leq$ 5 [22], which explains why hydrogen production of anaerobic bacteria, such as *Clostridium*, ceased at pH 4.5–5.0 with different superfluous substrates [13,23–25]. Similarly, hydrogen production in W12–W15 ceased within pH 4.6–4.9 in this study [**Fig. 2(C)**]. Inhibition of Pfk activity at an acidic pH should end the EMP pathway earlier and result in a high concentration of residual sucrose in W14 and W15.

Inactivation of butyrate formation pathway likely resulted in higher NADH/NAD^+ in W14 and W15. Three pathways are proposed to convert NADH to hydrogen in anaerobic bacteria: (i) NADH–ferredoxin reductase and hydrogenase [26], (ii) butyryl-CoA dehydrogenase (Bcd)/Etf complex (coupled ferredoxin and crotonyl coenzyme A reduction with NADH) and hydrogenase [27–29], and (iii) a bifurcating hydrogenase to oxidize NADH and ferredoxin simultaneously to produce H_2, which is found in *Thermotoga maritima* and some *Clostridium* species [18,30,31]. No homologs of three gene-encoding subunits of bifurcating hydrogenase were detected in the genomes of sequenced *C. perfringens* strains. Although three genes (cpe 2300, cpe 2299, and cpe 2298) encoding the three components of Bcd/Etf complex are detected in *C. perfringens* genome, blocking butyrate formation pathway resulted in the absence of Bcd/Etf complex. Only the first pathway of NADH-ferredoxin reductase and hydrogenase remained in W14 and W15. However, its efficiency might be very low and it might function only at very low partial pressures of hydrogen ($<$60Pa) as described previously [30,32], which might be the reason why W14 and W15 produce less hydrogen (**Table 2**).

Extra NADH may be consumed by lactate or ethanol formation pathways. Blocking butyrate biosynthetic pathway might change the redox balance in the addition of a putative congestion of C4 pathway which in turn leads to an induction of ethanol and lactate production instead of acetate formation in *C. acetobutylicum* [33,34]. In W14, due to the inactivation of lactate and butyrate formation pathways, the extra NADH was likely consumed only during ethanol formation, and thus the ethanol yield increased significantly when compared with W12 and W13 [**Fig. 2(I)**]. In W15, both lactate and ethanol formation pathways compete for NADH; however, the higher NADH/NAD^+ ratio activates

Ldh [35], and thus the lactate concentration increased more quickly than ethanol [**Fig. 2(H,I)**].

The increase in residual sucrose and the reduced levels of NADH conversion to hydrogen in W14 and W15 may directly give rise to lower hydrogen yield. According to the variation of metabolites in W12 and its three mutants (**Table 2, Fig. 2**), among all enzymes involved in the oxidization of NADH, the order of affinity to substrate NADH in *C. perfringens* W12 might be: Ldh≥Hdb≥Bcd, EtfA and EtfB complex>AdhE>>NADH−ferredoxin reductase. It may be possible to increase hydrogen yield in butyrate formation pathway-inactivated mutants by introducing more efficient NADH−ferredoxin reductase or bifurcating hydrogenase, which may convert NADH directly into hydrogen.

Blocking butyrate formation pathway up-regulates the expression of five genes involved in butyrate formation in W14 at transcriptional and translational levels. In most saccharolytic *Clostridia*, the cell adjusts the fraction of acetyl-CoA, which converts to acetate and butyrate to maintain redox balance [36]. As a normal response to redox unbalance, cells might alter the activity or the expression of proteins involved in reducing product formation, which explains the increased expression of five butyrate formation related proteins. However, variations in Adh and AhdE protein levels were not observed in 2-DE. It was speculated that the expression of *adh* and/or *adhE* was very low and/or they did not convert acetyl-CoA to ethanol, as reported in *C. acetobutylicum* [37]. Instead, the bacterium relied on ethanol synthesis under certain physiological conditions, similar to strains W14 and W15.

In summary, EtfA/B and Bcd might play a major role in converting NADH into hydrogen in *C. perfringens*. Thus, blocking butyrate formation pathway in W12 or W13 significantly decreased hydrogen production. Our results suggest that the substrate affinities of the enzymes involved in the oxidization of NADH in *C. perfringens* W12 might be Ldh≥Hdb≥Bcd, EtfA and EtfB complex> AdhE>> NADH−ferredoxin reductase and that *C. perfringens* prefers butyrate or lactate formation than ethanol to release the reductive ability of glycolysis.

Funding

This work was supported by a grant form the National Natural Science Foundation of China (31070098).

References

1 Hallenbeck PC and Ghosh D. Advances in fermentative biohydrogen production: the way forward? Trends Biotechnol 2009, 27: 287−297.
2 Liu XM, Ren NQ, Song FN, Yang CP and Wang AJ. Recent advances in fermentative biohydrogen production. Prog Nat Sci 2008, 18: 253−258.
3 Maeda T, Sanchez-Torres V and Wood TK. Enhanced hydrogen production from glucose by metabolically engineered Escherichia coli. Appl Microbiol Biot 2007, 77: 879−890.
4 Zhao HX, Ma K, Lu Y, Zhang C, Wang LY and Xing XH. Cloning and knockout of formate hydrogen lyase and H-2-uptake hydrogenase genes in *Enterobacter aerogenes* for enhanced hydrogen production. Int J Hydrogen Energ 2009, 34: 186−194.
5 Hallenbeck PC. Fundamentals of the fermentative production of hydrogen. Water Sci Technol 2005, 52: 21−29.
6 Evvyernie D, Yamazaki S, Morimoto K, Karita S, Kimura T, Sakka K and Ohmiya K. Identification and characterization of Clostridium *paraputrificum* M-21, a chitinolytic, mesophilic and hydrogen-producing bacterium. J Biosci Bioeng 2000, 89: 596−601.
7 Yoshida A, Nishimura T, Kawaguchi H, Inui M and Yukawa H. Enhanced hydrogen production from glucose using ldh- and frd-inactivated *Escherichia coli* strains. Appl Microbiol Biot 2006, 73: 67−72.
8 Zhu JB, Long MN, Xu FC, Wu XB and Xu HJ. Enhanced hydrogen production by insertional inactivation of adhE gene in *Klebsiella oxytoca* HP1. Chinese Sci Bull 2007, 52: 492−496.
9 Kumar N, Ghosh A and Das D. Redirection of biochemical pathways for the enhancement of H-2 production by *Enterobacter cloacae*. Biotechnol Lett 2001, 23: 537−541.
10 Morimoto K, Kimura T, Sakka K and Ohmiya K. Overexpression of a hydrogenase gene in *Clostridium paraputrificum* to enhance hydrogen gas production. Fems Microbiol Lett 2005, 246: 229−234.
11 Liu X, Zhu Y and Yang ST. Construction and characterization of ack deleted mutant of *Clostridium tyrobutyricum* for enhanced butyric acid and hydrogen production. Biotechnol Progr 2006, 22: 1265−1275.
12 Liu XG, Zhu Y and Yang ST. Butyric acid and hydrogen production by *Clostridium tyrobutyricum* ATCC 25755 and mutants. Enzyme Microb Tech 2006, 38: 521−528.
13 Wang R, Zong W, Qian C, Wei Y, Yu R and Zhou Z. Isolation of *Clostridium perfringens* strain W11 and optimization of its biohydrogen production by genetic modification. Int J Hydrogen Energ 2011, 36: 12159−12167.
14 Shao L, Hu S, Yang Y, Gu Y, Chen J, Yang Y and Jiang W, *et al*. Targeted gene disruption by use of a group II intron (targetron) vector in *Clostridium acetobutylicum*. Cell Res 2007, 17: 963−965.
15 Jiang Y, Xu CM, Dong F, Yang YL, Jiang WH and Yang S. Disruption of the acetoacetate decarboxylase gene in solvent-producing *Clostridium acetobutylicum* increases the butanol ratio. Metab Eng 2009, 11: 284−291.
16 Mao SM, Luo YAM, Zhang TR, Li JS, Bao GAH, Zhu Y and Chen ZG, *et al*. Proteome reference map and comparative proteomic analysis between a wild type *Clostridium acetobutylicum* DSM 1731 and its mutant with enhanced butanol tolerance and butanol yield. J Proteome Res 2010, 9: 3046−3061.
17 Li X, Liu T, Wu Y, Zhao G and Zhou Z. Derepressive effect of NH4+ on hydrogen production by deleting the glnA1 gene in *Rhodobacter sphaeroides*. Biotechnol Bioeng 2010, 106: 564−572.
18 Cai G, Jin B, Saint C and Monis P. Genetic manipulation of butyrate formation pathways in *Clostridium butyricum*. J Biotechnol 2011, 155: 269−274.
19 Hellinga HW and Evans PR. Mutations in the active site of *Escherichia coli* phosphofructokinase. Nature 1987, 327: 437−439.
20 Trivedi B and Danforth WH. Effect of pH on the kinetics of frog muscle phosphofructokinase. J Biol Chem 1966, 241: 4110−4112.
21 Ruminot I, Gutierrez R, Pena-Munzenmayer G, Anazco C, Sotelo-Hitschfeld T, Lerchundi R and Niemeyer MI, *et al*. NBCe1 mediates the acute stimulation of astrocytic glycolysis by extracellular K+. J Neurosci 2011, 31: 14264−14271.
22 Gheshlaghi R, Scharer JM, Moo-Young M and Chou CP. Metabolic pathways of clostridia for producing butanol. Biotechnol Adv 2009, 27: 764−781.

23 Lin PY, Whang LM, Wu YR, Ren WJ, Hsiao CJ, Li SL and Chang JS. Biological hydrogen production of the genus *Clostridium*: metabolic study and mathematical model simulation. Int J Hydrogen Energ 2007, 32: 1728–1735.
24 Chen WM, Tseng ZJ, Lee KS and Chang JS. Fermentative hydrogen production with *Clostridium butyricum* CGS5 isolated from anaerobic sewage sludge. Int J Hydrogen Energ 2005, 30: 1063–1070.
25 Davila-Vazquez G, Alatriste-Mondragon F, de Leon-Rodriguez A and Razo-Flores E. Fermentative hydrogen production in batch experiments using lactose, cheese whey and glucose: influence of initial substrate concentration and pH. Int J Hydrogen Energ 2008, 33: 4989–4997.
26 Vardar-Schara G, Maeda T and Wood TK. Metabolically engineered bacteria for producing hydrogen via fermentation. Microb Biotechnol 2008, 1: 107–125.
27 Herrmann G, Jayamani E, Mai G and Buckel W. Energy conservation via electron-transferring flavoprotein in anaerobic bacteria. J Bacteriol 2008, 190: 784–791.
28 Li F, Hinderberger J, Seedorf H, Zhang J, Buckel W and Thauer RK. Coupled ferredoxin and crotonyl coenzyme a (CoA) reduction with NADH catalyzed by the butyryl-CoA dehydrogenase/Etf complex from *Clostridium kluyveri*. J Bacteriol 2008, 190: 843–850.
29 Hetzel M, Brock M, Selmer T, Pierik AJ, Golding BT and Buckel W. Acryloyl-CoA reductase from *Clostridium propionicumi*—an enzyme complex of propionyl-CoA dehydrogenase and electron-transferring flavoprotein. Eur J Biochem 2003, 270: 902–910.
30 Schut GJ and Adams MWW. The iron-hydrogenase of thermotoga maritima utilizes ferredoxin and NADH synergistically: a new perspective on anaerobic hydrogen production. J Bacteriol 2009, 191: 4451–4457.
31 Calusinska M, Happe T, Joris B and Wilmotte A. The surprising diversity of clostridial hydrogenases: a comparative genomic perspective. Microbiol Sgm 2010, 156: 1575–1588.
32 Mandal B, Nath K and Das D. Improvement of biohydrogen production under decreased partial pressure of H-2 by *Enterobacter cloacae*. Biotechnol Lett 2006, 28: 831–835.
33 Lehmann D, Radomski N and Lütke-Eversloh T. New insights into the butyric acid metabolism of *Clostridium acetobutylicum*. Appl Microbiol Biot 2012, 96: 1325–1339.
34 Cooksley CM, Zhang Y, Wang H, Redl S, Winzer K and Minton NP. Targeted mutagenesis of the *Clostridium acetobutylicum* acetone-butanol-ethanol fermentation pathway. Metab Eng 2012, 14: 630–641.
35 Garrigues C, Mercade M, Cocaign-Bousquet M, Lindley ND and Loubiere P. Regulation of pyruvate metabolism in *Lactococcus lactis* depends on the imbalance between catabolism and anabolism. Biotechnol Bioeng 2001, 74: 108–115.
36 Thauer RK, Jungermann K and Decker K. Energy conservation in *Chemotropic anaerobic* bacteria. Bacteriol Rev 1977, 41: 100–180.
37 Lehmann D and Lutke-Eversloh T. Switching *Clostridium acetobutylicum* to an ethanol producer by disruption of the butyrate/butanol fermentative pathway. Metab Eng 2011, 13: 464–473.